The 2012 World Congress on
Advances in Civil, Environmental, and Materials Research (ACEM' 12)
Seoul, Korea, August 26-30, 2012

Wind Pressures on Solar Panels Mounted on Residential Homes

Aly Mousaad ALY[1)] and Girma BITSUAMLAK[2)]

[1] Research Fellow, WindEEE Research Institute, Department of Civil and Environmental Engineering, Western University, Boundary Layer Wind Tunnel Laboratory, London, ON, Canada, N6A 5B9, aalysaye@UWO.ca

[2] Associate Professor, Associate Director WindEEE Research Institute, Department of Civil and Environmental Engineering, Western University , Boundary Layer Wind Tunnel Laboratory Rm. 105, London, ON, Canada, N6A 5B9, gbitsuam@UWO.ca

ABSTRACT

The existing literature has less comprehensive data for the evaluation of the wind loads on the solar panels mounted on residential buildings. Furthermore, there are no provisions in building codes and standards to guide the design of these types of structures for wind. To alleviate this problem, this paper presents wind load analysis on solar panel modules mounted on low-rise buildings with gable roofs that has two different slopes. Wind loads on the solar panels mounted on different zones of the roofs are systematically investigated in a boundary layer wind tunnel for different wind directions. The aim of this study is to contribute with useful information for the estimation and codification of wind loads on the solar panels.

1. INTRODUCTION

There is a renewed interest in using solar panels (photovoltaic/thermal) as a renewable source of energy. However, a cost effective and safe design that will make such energy generation alternative competitive with traditional energy resources is still remains a challenge. A safe, yet economical, design of the solar panels for wind requires accurate information on the estimation of the wind loads, among other factors, which can affect significantly the construction cost. Since these structures are relatively new, wind loads on solar panels are hardly covered by current design standards.

Solar panels for residential building applications are typically installed on roofs, the most wind vulnerable region. Wind produces high negative and positive pressures on roof surface which may cause failure to its components/claddings and/or the roof main structure (Bienkiewicz and Sun, 1992, 1997; Aly et al. 2012). In certain zones of the roof, (i.e., windward edges, corners, and eaves), wind flow may cause large drop in air pressure above the panel's surface. The resultant pressure difference on individual panel (net pressure, which is the difference between top and bottom pressures) creates an uplift force which may result in roof failure, panel's failure and airborne missiles. Being airborne missiles, solar panels may lead to successive failure to the surrounding building environment.

A number of studies have been developed for the estimation of the wind loads on roof-mounted solar panels (Ming et al., 2010; Shademan and Hangan, 2009; Geurts and Van Bentum, 2007; Kopp, et al. 2002). Radu et al. (1986) conducted Wind Tunnel tests on an array of solar panels mounted on top of a five-story residential building, and showed the significance of the sheltering effect from the building and the first row of solar collectors. Peterka et al. (1987) conducted a series of wind tests on an array of heliostats, and investigated the wind load reductions obtained from utilizing protective fences, as well as the sheltering effect from neighboring panels. Wood et al. (2001) conducted wind tunnel pressure tests on a scaled model of a large industrial building with solar panels mounted parallel to a flat roof. The study concluded that the orientation of a solar panel with respect to wind-flow and its proximity to the leading edge of the building had a significant effect when designing a solar panel system. Kopp et al. (2002) conducted Wind Tunnel tests to study aerodynamically induced torque loads on solar panel array system. Based on the observations gathered, a large peak torque resulted from a strong vortex shedding, in addition to turbulence in the incoming wind-flow.

The existing literature has less than comprehensive data for the evaluation of the wind loads on the solar panels. Furthermore, there are no provisions in building codes and standards to guide the design of these types of structures for wind. As a result, structural engineers and practitioners adopt provisions that were established for low-rise buildings, resulting in either conservative designs that overestimate the wind loads or unsafe structures (Barkaszi and O'Brien, 2010).

The purpose of this study is to assess the aerodynamic wind loads acting on solar panel modules mounted on low-rise residential homes. Wind loads on solar panels mounted on different critical zones of gable roofs are systematically investigated for different wind directions.

2. Methodology

Solar panel modules: three sizes of solar panels are considered in the present boundary layer wind tunnel study, namely small (3 ft x 5 ft or 0.9144 m x 1.524 m), medium (5 ft x 8 ft or 1.524 m x 2.4384 m) and big (5 ft x 9 ft or 1.524 m x 2.7432 m). The tap layout on top and bottom surfaces of the solar panel modules is shown in Fig. 1. Fig. 1 shows tap layout and tributary areas for three solar panel test models: (a) small (S), (b) medium (M) and (c) big (B). In the figure, hollow circles designate locations of top and bottom pressure taps and solid circles designate centers of the tributary areas. Tributary boundaries are indicated by thin lines.

All of the modules were scaled 1:15 and mounted on gable roofs with two different slopes. Two roofs with similar dimensions but different slopes (3:12 and 5:12) were used. The dimension of a roof scaled 1:15, as well as the building footage, are shown in Fig. 2. The roof mean height at small-scale is 11.2 inches (0.2845 m). A gable roof with a slope of 3:12 (14^{o}) was first instrumented with pressure taps for external pressure assessment. Second, the modules were mounted on a quarter of the building as shown in Fig. 2. The rest of the roof was covered by dummy modules (for aerodynamic similarity purposes) according to the configuration type. Note that only quarter of the roof was instrumented due to symmetry. Four different arrangements of

the modules were tested. The arrangements are: (1) horizontal arrangement where the modules are covering the entire roof, with some gab between the rows, this arrangement is called “configuration H1” (Fig. 2-a); (2) vertical arrangement where the modules are covering the entire roof without any significant gab (configuration V1 as shown in Fig. 2-b); (3) horizontal arrangement where the critical roof corner zones close to the eave, ridge and gable end edges are avoided and some gab between the rows exist (configuration H2 as shown in Fig. 2-c); (4) vertical arrangement where the roof critical corner zones are avoided and some gab between the modules was permitted (configuration V2 as shown in Fig. 2-d). All of the modules are placed parallel to the main roof surface with a full-scale gab of 6 inches (0.1524 m). The effect of roof slope was studied by considering two roofs with different slopes (3:12 and 5:12).

Wind profile: an open country wind profile was simulated at RWDI’s boundary layer wind tunnel in Miramar, Florida. The mean wind speed, turbulence intensity and integral length scales of the along wind velocity component are shown in Fig. 3. The generated wind spectrum is plotted in Fig. 4 in comparison with the Florida Coastal Monitoring Program (FCMP) and the von Karaman spectra taken from the literature (Masters, 2004; Holmes, 2001). Wind pressure data over the top and bottom surfaces of the modules instrumented in Fig. 2 are collected for a time period of 90 s at a sampling rate of 512 Hz. The velocity scale was assumed to be 4. For a geometric length scale of 15 the time scale is 3.75. This means that the 90-s test period in the laboratory represents 5.625 minutes at full-scale. The mean wind speed over 3-s period was used for pressure data normalization. The 3-s wind speed was obtained using the Durst curve (ASCE 7-2005 Appendix C).

Pressure coefficients: At the location of each pressure tap, the time history of the pressure coefficient, $Cp(t)$, is obtained from the time history of the measured differential pressure, $p(t)$, as

$$Cp(t) = \frac{p(t)}{\frac{1}{2}\rho U_{3s}^2} \tag{1}$$

where ρ is the air density at the time of the test and U_{3s} is the highest observed peak 3-s wind speed measured at the mean height of the roof (0.2845 m) over a time period of 90 s.

In designing the solar panels, it is necessary to determine the net pressure on the individual modules. The net pressure coefficient at any location, $Cp_{net}(t)$, is the simultaneous difference between the top pressure coefficient at the top surface, $Cp_{top}(t)$, and the pressure coefficient at the bottom surface, $Cp_{bot}(t)$, at the same locations

$$Cp_{net}(t) = Cp_{top}(t) - Cp_{bot}(t). \tag{2}$$

The minimum and maximum pressure coefficient values ($Cp_{\min}$ and $Cp_{\max}$) may be obtained from the measured pressure time histories. Nevertheless, these observed peaks can exhibit wide variability from one realization to another due to the highly fluctuating nature of wind pressures. This means that significant differences might be expected in the peak values of pressure time series obtained from several different

tests under nominally identical conditions. Therefore it is generally preferable to use a more stable estimator for the expected peaks. To remove the uncertainties inherent in the randomness of the peaks, probabilistic analyses were performed using an automated procedure developed by Sadek and Simiu (2002) for obtaining statistics of pressure peaks from observed pressure time histories. Because estimates obtained from this approach are based on the entire information contained in the time series, they are more stable than estimates based on observed peaks (Aly et al., 2012).

3. Results and discussions

Fig. 5 shows minimum external pressure coefficient's (Cp_{min}) distribution over a bare gable roof with a slope of 3:12 (14^o). The figure shows that at regions close to the roof edge and ridge, the roof experiences higher suction pressures. Fig. 6 shows minimum net pressure coefficient's (Cp_{min}) distribution over a group of solar panel modules arranged in "configuration H1" and mounted on a gable roof with a slope of 3:12 (14^o). The figure shows that some localized net pressures on solar panel modules mounted on the whole roof can be slightly higher than the external pressures on a bare roof (at regions very close to the roof's edge). However, by moving away from the edge the net pressure is less than the external pressure on the bare roof. Fig. 7 shows minimum net pressure coefficient's (Cp_{min}) distribution over a group of solar panel modules arranged in "configuration V1". Similar to "configuration H1", the net pressure over the solar panel mounted close to the edge is slightly higher than the case of the bare roof and the net pressure is less than the external pressure at locations away from the roof edge. The minimum net pressure coefficient's (Cp_{min}) distribution over a group of solar panel modules arranged in "configuration H2" are illustrated in Fig. 8. By avoiding the critical roof zones, i.e. close to the roof edges, corners, and the ridge, solar panel modules are subjected to net uplift pressures that are generally lower than the external uplift pressure on the bare roof. This configuration may be recommended for lower design wind loads on the solar panel modules. Minimum net pressure coefficient's (Cp_{min}) distribution over a group of solar panel modules arranged in "configuration V2" are shown in Fig. 9. Similar to "configuration H2", the net pressure on the solar panels is generally lower than the external pressure on the bare roof which makes this configuration favorable for solar panel mounting on gable roofs with slope 3:12 (14^o).

Net pressure coefficients over roof zones defined in the ASCE 7-2005 (2006) for bare roof are also calculated for comparison reasons. Fig. 10 shows roof zones (3, 2 and 1) used for comparisons with data provided in the ASCE-2005 (Figure 6-11C of the standard) for claddings, and roof zones (2E and 2-st) used for comparisons with data provided in ASCE 7-2005 (Figure 6-10 of the standard) for the main force resisting system.

Table 1 lists net pressure coefficients for the solar panel modules mounted over roof zones (3, 2 and 1) and comparisons with data provided by the ASCE-2005 (Figure 6-11C of the standard) for claddings. It is shown that the external minimum pressure coefficients estimated over the bare roof (slope 3:12) are relatively higher than the net pressure coefficients estimated over solar panels mounted on the corresponding zones. For zones 3, the ASCE standard predicts higher minimum pressure coefficients by a factor of about 32%. Minimum pressure coefficients over the solar panel modules in

zone 2 are dependent on the configuration (horizontal or vertical). The horizontal configuration of solar panels in zone 2 is in agreement with the minimum pressures predicted by the ASCE standard over a bare roof with an overhang. However, net pressures over panels in zone 2 with "configuration V1" are relatively higher than those estimated in "configuration H1." This may be due to the effect of the gap between the panels (20% of the panel's width) that exist in "configuration H1" (see Fig. 2-a). This means that the ASCE standard underestimates the minimum pressure on zone 2 for the solar panels mounted with no significant spacing between the modules by a percentage of 34%. In other words, a factor of 1.34 might be useful to make use of the data provided in the ASCE standard for gable roofs. It worth noting that Banks (2007) recommends an uncertainty factor of 1.4, incase data provided by ASCE 7 are used. The minimum design pressure predicted by the standard on modules in zone 1 is about two times the actual net minimum pressures.

In Table 1, it is shown that the maximum pressure predicted by the standard over modules in zones 3 and 2 are generally lower than the net pressures by a factor of 50% to 60%. The standard overestimates the maximum net pressures for the modules in zone 1 by a factor of 25 to 47%.

Table 2 lists net pressure coefficients over roof zones (2E and 2-st) for solar panels mounted on a gable roof with a slope of 3:12 (14^o) and comparisons with data provided by the ASCE 7-2005 (Figure 6-10 of the standard) for the main force resisting system. It is shown that the ASCE 7-2005 standard may be used for estimating the net uplifts loads acting on solar panel modules mounted on a gable roof with slope of 14^o for the main force resisting system.

In order to estimate the wind loads on each individual solar panel module, the maximum and minimum net pressures (GCP+ and GCP-) on each module are calculated for different wind direction angles (from 0^o to 350^o with an increment of 10^o). Fig. 11 shows the net pressure coefficients on panels mounted on a gable roof (slope 3:12) for different wind direction angles. From these data, and for all of the solar panel modules mounted on gable roofs with different slopes, one can estimate GCP+ and GCP- for design purposes. For comparisons with the ASCE standard, one may consider GCP+ and GCP- provided in ASCE-2005 (Figure 6-11C of the standard) for claddings and according to the location of the panel on the roof, GCP+ and GCP- may be calculated through interpolation, for example, a solar panel with an area "A" in two zones (2 and 1) may have an area "A1" in zone 1 and the rest of the area "A2" in zone 2. The area average minimum or maximum pressure coefficients (GCP+ or GCP-) may be calculated as follows:

$$GCP^{+} = \frac{GCP_1^{+} \times A_1 + GCP_2^{+} \times A_2}{A_1 + A_2}. \qquad (3)$$

Figures 12-15 show maximum and minimum net pressure coefficients on solar panel modules mounted on gable roofs with slopes 3:12 and 5:12 and comparisons with corresponding pressure coefficients obtained from external pressures on a bare gable roof provided in the ASCE 7-2005 standard. The figures show that solar panel modules are subjected to lower net maximum pressures than the positive pressures on a bare roof predicted by the standard.

Fig. 12 shows maximum and minimum net pressure coefficients on solar panel modules mounted on gable roofs with slopes 3:12 and 5:12 in “configuration H1” of Fig. 2 and comparisons with pressure coefficients obtained from external pressure on a bare gable roof predicted by the ASCE 7-2005 standard. It is shown that the external pressure on a gable roof with slope (from 7^o to 27^o) provided in the ASCE standard may overestimate the net pressure over modules mounted at regions close to the corners and the ridge (B2, M1 and M3 in Fig. 2). This may be because of the contribution of the bottom pressure to the net pressure on the panels. It worth noting that solar panels mounted on a roof with slope 5:12 are subjected to lower negative pressure than the corresponding panels mounted on roof with a slope of 3:12.

Fig. 13 shows maximum and minimum pressure coefficients on solar panel modules mounted on gable roofs with slopes 3:12 and 5:12 in “configuration V1” of Fig. 2 and comparisons with external pressure coefficients for a bare gable roof provided by the ASCE 7-2005 standard. Similar to “configuration H1”, it is shown that the ASCE standard may overestimate the wind loads on the solar panel modules. It is also shown that solar panels mounted on a gable roof with slope 3:12 are subjected to higher negative pressures than those mounted on a gable roof with slope 5:12.

Fig. 14 shows maximum and minimum pressure coefficients on solar panel modules mounted on gable roofs with slopes 3:12 and 5:12 in “configuration H2” of Fig. 2 and comparisons with corresponding loads obtained from external pressure on a bare gable roof predicted by the ASCE 7-2005 standard. It is shown that by avoiding the zones close to the roof edges and ridge, the net negative pressures on the solar panel modules are reduced (w.r.t configurations H1 and V1).

Fig. 15 shows maximum and minimum net pressure coefficients on solar panel modules mounted on gable roofs with slopes 3:12 and 5:12 in “configuration V2” of Fig. 2 and comparisons with corresponding loads obtained from external pressure on a bare gable roof predicted by the ASCE 7-2005 standard. It is shown that the net negative pressure acting on solar panels away from the roof edges and ridge is generally lower than the case when the whole roof was covered by panels. This means avoiding the roof critical zones is useful in reducing the net negative pressures acting on the solar panel modules. However, the value estimated on modules S1 and S2 are higher than the corresponding values predicted by the code at the same zone. This may be due to the effect of a secondary roof formed over the main roof where the edges of the new roof are generally critical. It worth noting that this effect is shown for smaller modules (“S1” and “S2”) and not the medium size ones (“M1”-“M5”) because of geometry, i.e. smaller modules are located mostly in the critical zone of the secondary roof rather than the medium ones.

CONCLUSION

The paper investigated wind effects on roof-mounted solar panels with an aim to reduce the overall construction costs and to examine possibility of using design codes applicable to gable roofs. The main contributions of the current study are summarized as follows:

1. The net pressure distribution (design load) for solar panels mounted on a gable roof, considered in the present study, is significantly different from the external pressure distribution over a bare roof with same geometry.
2. In an effort to make use of the available pressure coefficients in ASCE 7-2005 standard on a gable roof for estimating design wind pressures of roof mounted solar panels, the following was noticed.
   a. For cladding loads: Solar panels mounted close to roof corners (zone 3) are generally subjected to lower net pressures than the external pressure provided by ASCE 7-2005 for a bare roof. The code over estimates the minimum pressures by a factor of 32%. Panels mounted at roof edges and away from corners (zone 2) are generally subjected to lower net pressures than the external pressure provided by ASCE 7-2005 for a bare roof. The standard predicts very similar values on modules mounted with a gap between the rows (20% of the panel's width). Nevertheless, the standard underestimates the minimum pressures by a factor of 34% when the gap was eliminated. The minimum design pressure predicted by the standard on modules in zone 1 is about two times the minimum net pressure. The maximum pressure predicted by the standard over modules in zones 3 and 2 are generally lower than the net pressures by a factor of 50% to 60%. The standard overestimates the maximum net pressures on the modules installed in zone 1 by a factor of 25 to 47%.
   b. For the main force resisting system loads: The ASCE 7-2005 standard may be used for estimating the net uplifts loads acting on solar panel modules mounted on a gable roof with a slope of 14^{o}.

3. Aerodynamic pressures for the solar panels mounted on gable roofs are highly dependent on the roof slope and the panel's location as well as their configuration. Generally speaking, it may be recommended to avoid mounting the solar panels in zones located close to the roof edge, ridge, and corners as the wind loads are higher at these zones (zone 3 and 2). Solar panels mounted on a gable roof with a slope of 22.6^{o} are subjected to less minimum pressures than those on a gable roof with a slope of 14^{o}. The maximum pressure coefficients for the solar panels mounted on the two roofs considered are generally lower than the maximum external pressure coefficients provided in the ASCE 7-2005 standard.
4. Although avoiding the roof critical zones (3 and 2) is useful in reducing the net minimum pressures acting on the solar panel modules, solar panels mounted in zone 1 are subjected to higher suction at their outer edges. This may be due to the effect of a secondary roof formed over the main building's roof where the edges of the new roof are generally critical. These effects can be noticeable for small modules, however, for larger modules, the effect of the secondary roof is not significant.
5. The results of the current study provides practicing engineers and code officials with useful information for codification.

REFERENCES

ASCE 7-2005 (2006). Minimum design loads for buildings and other structures. ASCE Standard, ASCE/SEI 7-05, American Society of Civil Engineers, Virginia.

Aly, A.M., Bitsuamlak, G. and Gan Chowdhury, A., (2012), "Full-scale aerodynamic testing of a loose concrete roof paver system," Engineering Structures (in press).

Holmes, D.J. (2001), Wind Loading of Structures, Spon Press, London.

Masters, F. J., (2004). Measurement, modeling and simulation of ground-level tropical cyclone winds. PhD dissertation, University of Florida.

Sadek, F. and Simiu, E. (2002), "Peak non-Gaussian wind effects for database-assisted low-rise building design," Journal of Engineering Mechanics, ASCE, 128(5), 530-539.

Banks David. How to Calculate Wind Loads on Roof Mounted Solar Panels in the US. http://www.cppwind.com/services/renewable_energy/renewable_energy.html

Barkaszi S, O'Brien C (2010), "Wind Load Calculations for PV arrays," A report, Solar America Board for Codes and Standards, (www.solarabcs.org, June 2012).

Bienkiewicz, B. and Sun, Y. (1992), "Local wind loading on the roof of a low-rise building," Journal of Wind Engineering and Industrial Aerodynamics, 45, 11-24.

Bienkiewicz, B. and Sun, Y. (1997), "Wind loading and resistance of loose-laid roof paver systems," Journal of Wind Engineering and Industrial Aerodynamics, **72**, 401-410.

Geurts, C.P.W. and Van Bentum, C.A. (2007), "Wind loads on solar energy roofs," Heron, **52**(3), 201-222.

Kopp, G.A., Surry, D. and Chen, K. (2002), "Wind loads on a solar array," Wind and Structures, An International Journal, **5**(5), 393-406.

Ming, J., Liu, Z. and Zhang, Q. (2010), "Solar photovoltaic panels wind load testing and analysis," 2010 International Conference on Mechanic Automation and Control Engineering, MACE2010, June 26, 2010 - June 28, 2010.

Peterka, J.A., Bienkiewicz, B., Hosoya, N. and Cermak, J.E., (1987), "Heliostat mean wind load reduction," Energy **12**, 261-267.

Radu, A., Axinte, E. And Theohari, C., (1986), "Steady wind pressures on solar collectors on flat-roofed buildings," Journal of Wind Engineering and Industrial Aerodynamics, **23**, 249-258.

Shademan, M. and Hangan, H. (2009), "Wind Loading on Solar Panels at Different Inclination Angles," 11th American Conference on Wind Engineering, San Juan, Puerto Rico, June 22-26, 2009.

Wood, G.S., Denoon, R.O. and Kwok, K.C.S., (2001), "Wind loads on industrial solar panel arrays and supporting roof structure," Wind and Structures, An International Journal, **4**, 481-494.

Tables

Table 1 Net pressure coefficients over roof zones (3, 2 and 1) for solar panels mounted on a gable roof with a slope of 3:12 (14^o) and comparisons with data provided by the ASCE-2005 (Figure 6-11C of the standard) for claddings

	Zone 3		Zone 2		Zone 1	
Configuration	GCP+	GCP-	GCP+	GCP-	GCP+	GCP-
Wind tunnel						
H1	1.03	-2.78	1.22	-1.94	0.40	-0.32
V1	1.02	-2.83	1.16	-3.01	0.34	-0.42
H2	_	_	_	_	0.71	-0.34
V2	_	_	_	_	0.43	-0.22
Bare roof (slope = 14^o)	0.77	-4.14	0.56	-3.12	0.16	-0.96
ASCE bare roof (7^o < slope < 27^o)	0.50	-3.70	0.50	-2.00	0.50	-0.90

Table 2 Net pressure coefficients over roof zones (2E and 2-st) for solar panels mounted on a gable roof with a slope of 3:12 (14^o) and comparisons with data provided in the ASCE 7-2005 (Figure 6-10 of the standard) for the main force resisting system.

	Zone 2E		Zone 2	
Configuration	GCP+	GCP-	GCP+	GCP-
Wind tunnel				
H1	0.25	-1.03	0.47	-0.55
V1	0.40	-1.08	0.35	-0.68
H2	_	_	0.71	-0.42
V2	_	_	0.46	-0.35
ASCE Bare roof (7^o < slope < 27^o)	_	-1.07	_	-0.67

Figures

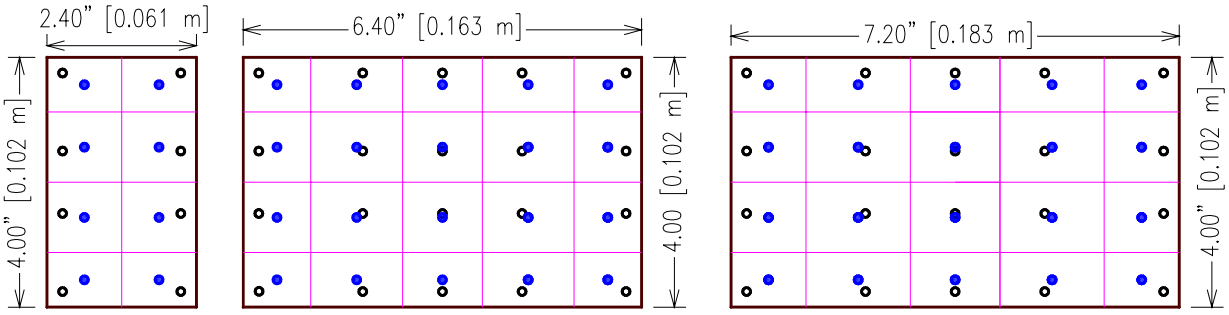

(a) Small (b) Medium (c) Big

Fig. 1 Tap layout and tributary areas for three solar panel test models: (a) small “S”, (b) medium “M” and (c) big “B”. Hollow circles designate locations of external and underneath pressure taps and solid circles designate centers of the tributary areas. Tributary boundaries are indicated by thin lines.

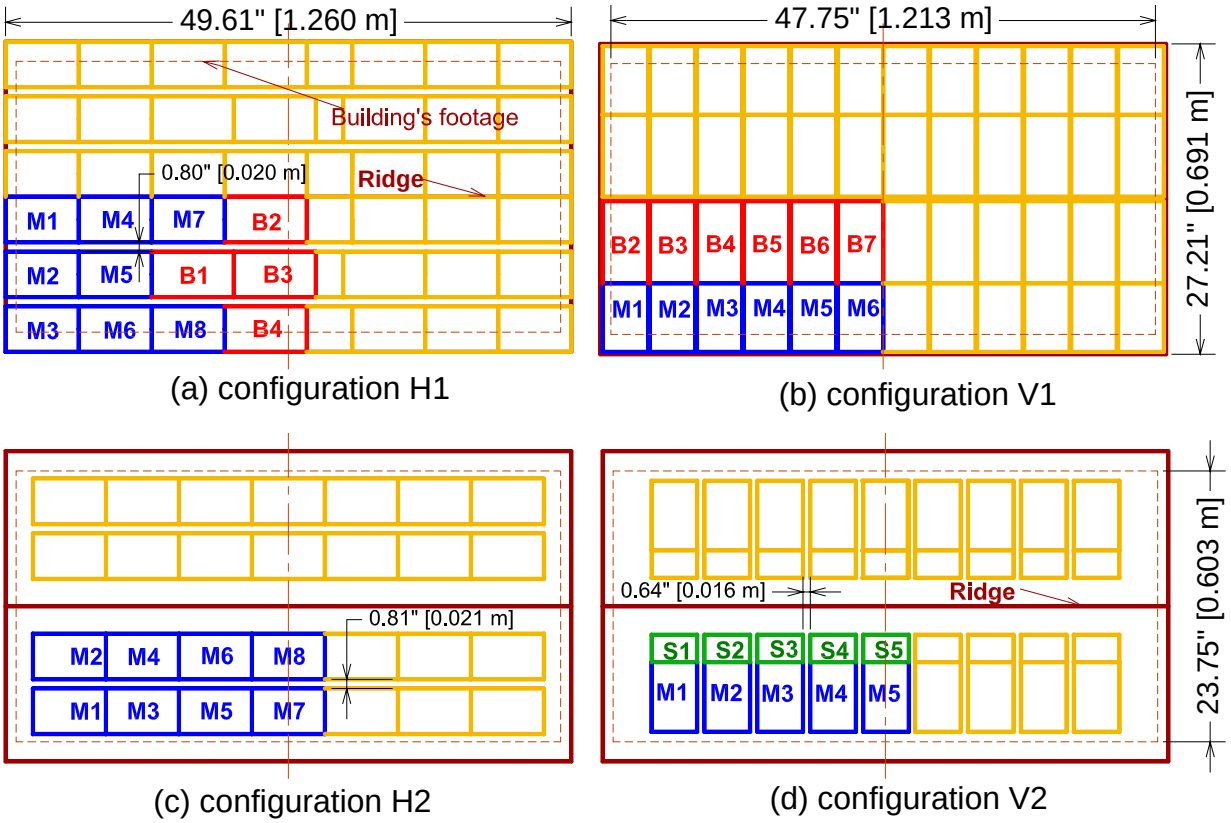

(a) configuration H1 (b) configuration V1

(c) configuration H2 (d) configuration V2

Fig. 2 Four different configurations of the solar panels were used: (a) horizontal configuration H1, (b) vertical configuration V1, (c) horizontal configuration H2 and (d) vertical configuration V2. The modules shown in Fig. 1 were instrumented with pressure taps and referred to as big “B”, medium “M” and small “S”. Note that only quarter of the roof was instrumented due to symmetry. Other modules are dummy and just presented for aerodynamic purposes.

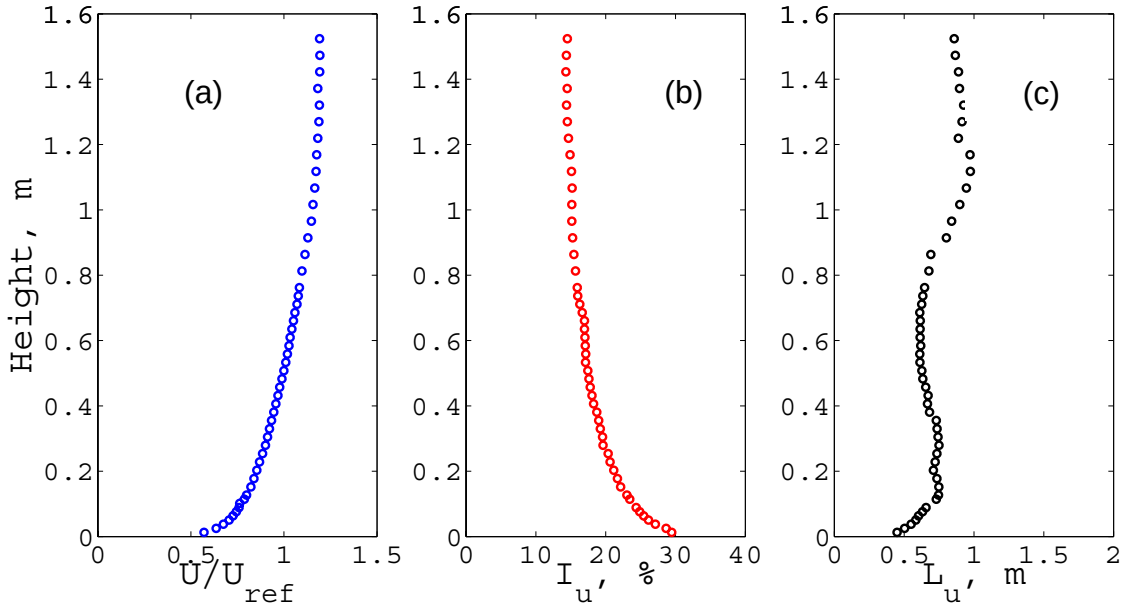

Fig. 3 Wind tunnel velocity characteristics: (a) mean wind speed profile, (b) turbulence intensity profile and (c) integral length scale. U is the along-wind velocity component.

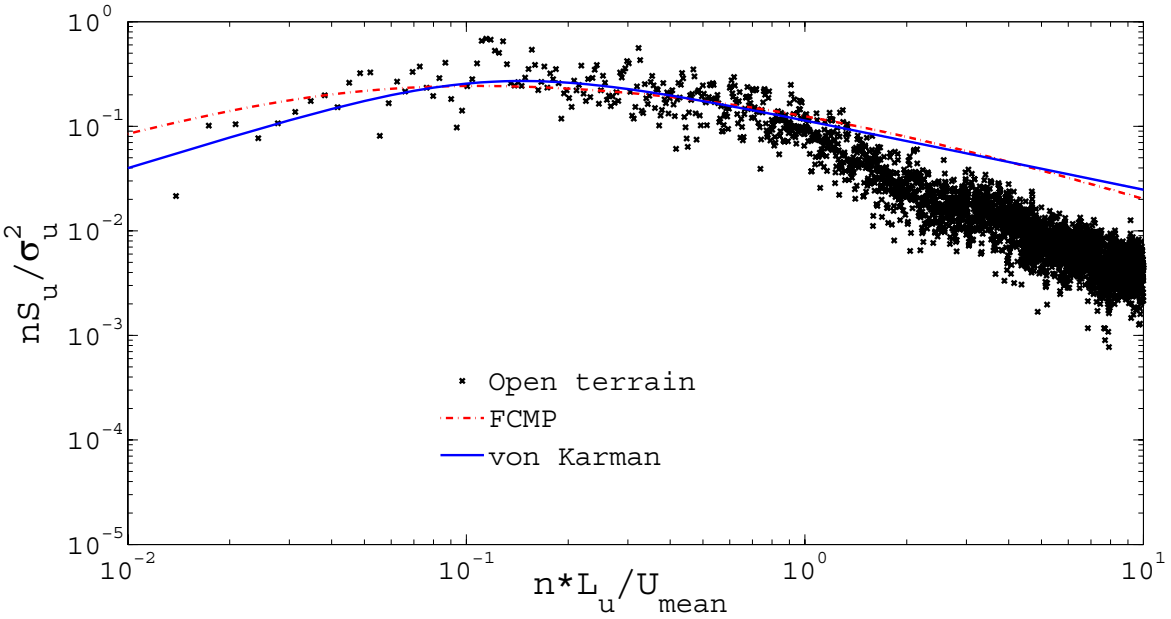

Fig. 4 Wind spectra of the along-wind velocity component (U) and comparison with the literature.

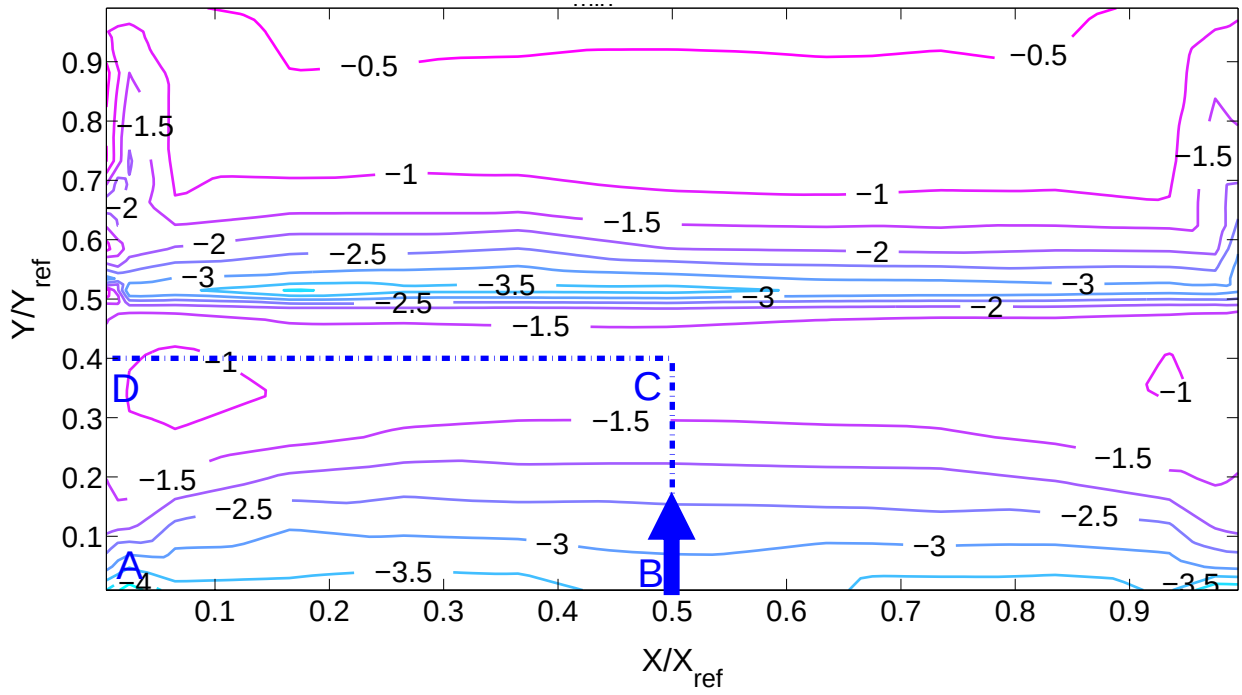

Fig. 5 Minimum external pressure coefficient's (Cp_{min}) distribution over a bare gable roof with slope 3:12(14^o); the arrow shows wind direction. Y_{ref} and X_{ref} are width and length of the roof, respectively.

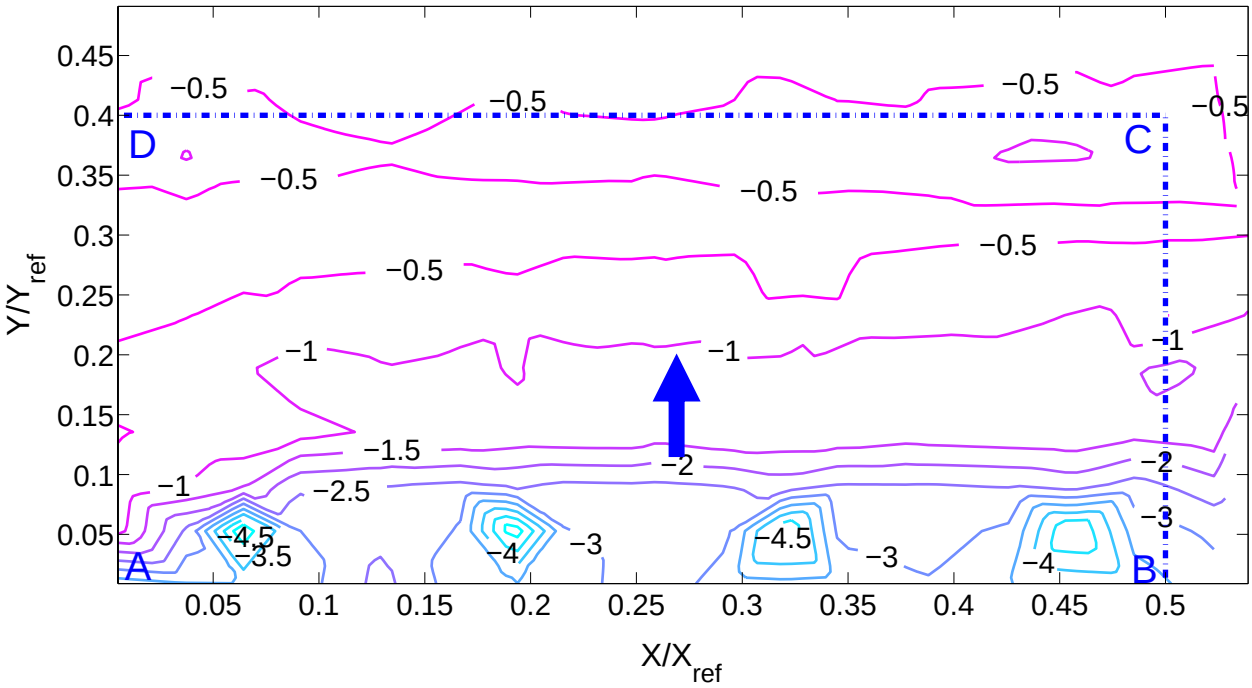

Fig. 6 Minimum net pressure coefficient's (Cp_{min}) distribution over a group of solar panel modules arranged in "configuration H1" and mounted on a gable roof with slope 3:12 (14^o); the arrow shows wind direction. Y_{ref} and X_{ref} are the width and the length of the roof, respectively.

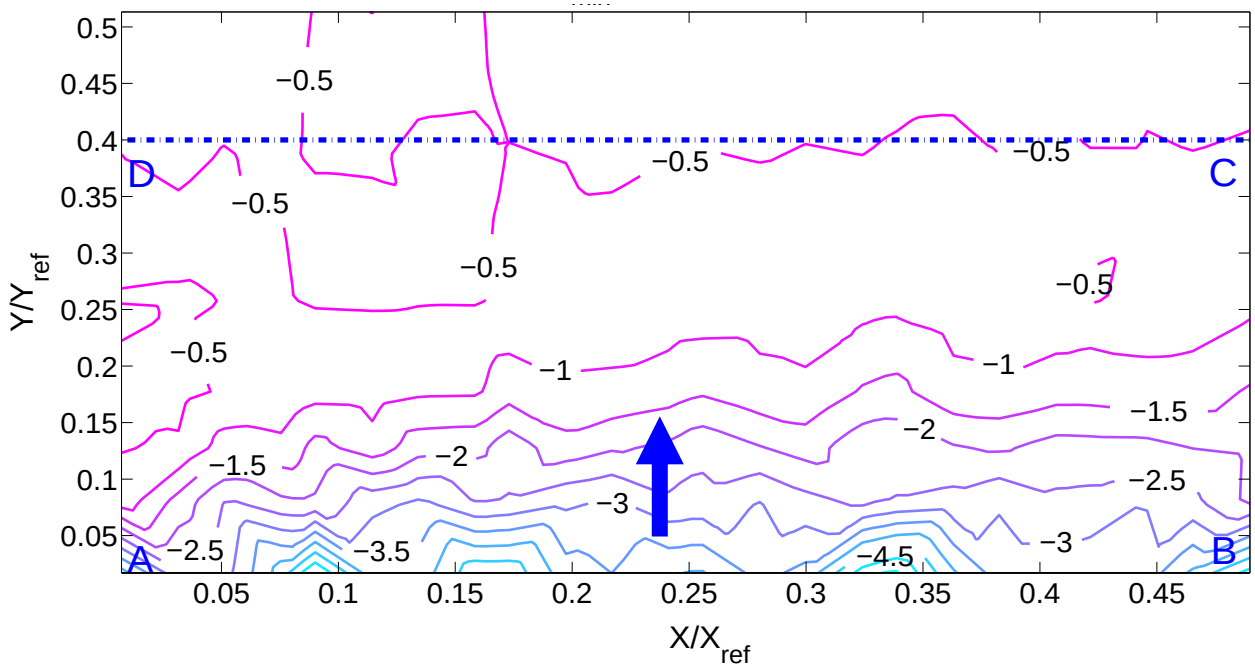

Fig. 7 Minimum net pressure coefficient's (Cp_{min}) distribution over a group of solar panel modules arranged in "configuration V1" and mounted on a gable roof with slope 3:12 (14^o); the arrow shows wind direction. Y_{ref} and X_{ref} are the width and the length of the roof, respectively.

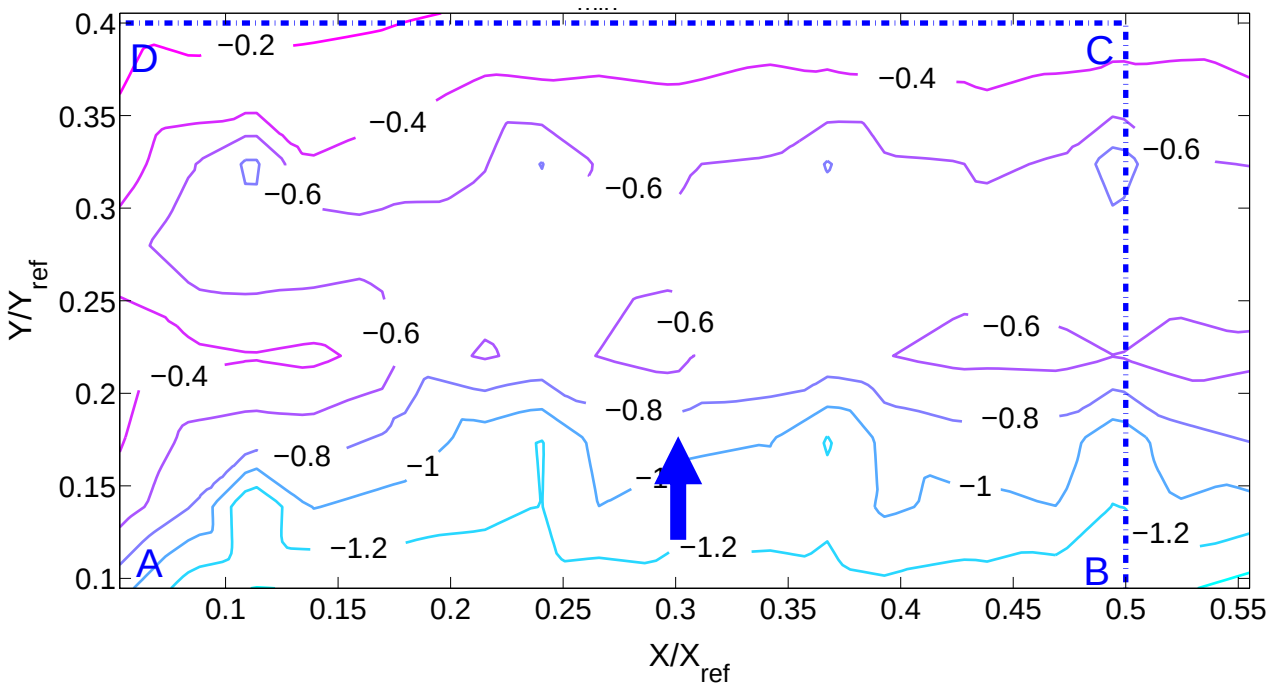

Fig. 8 Minimum net pressure coefficient's (Cp_{min}) distribution over a group of solar panel modules arranged in "configuration H2" and mounted on a gable roof with slope 3:12 (14^o); the arrow shows wind direction. Y_{ref} and X_{ref} are the width and the length of the roof, respectively.

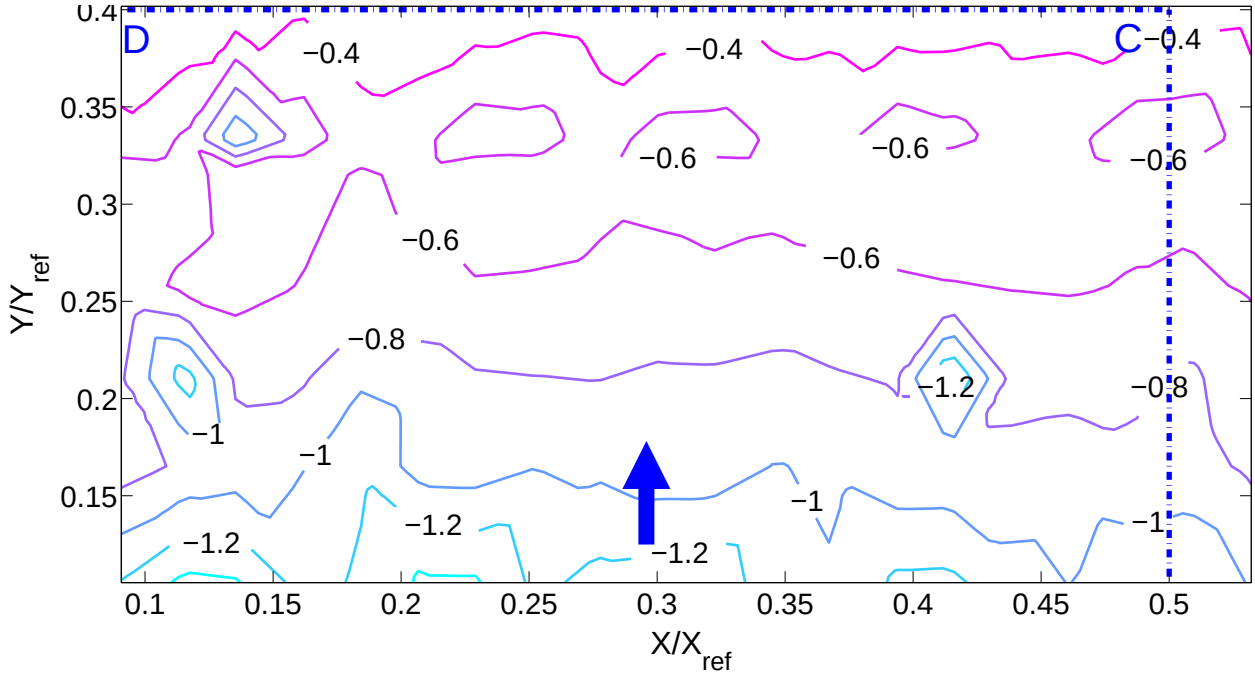

Fig. 9 Minimum net pressure coefficient's (Cp_{min}) distribution over a group of solar panel modules arranged in "configuration V2" and mounted on a gable roof with slope 3:12 (14^{o}); the arrow shows wind direction. Y_{ref} and X_{ref} are the width and the length of the roof, respectively.

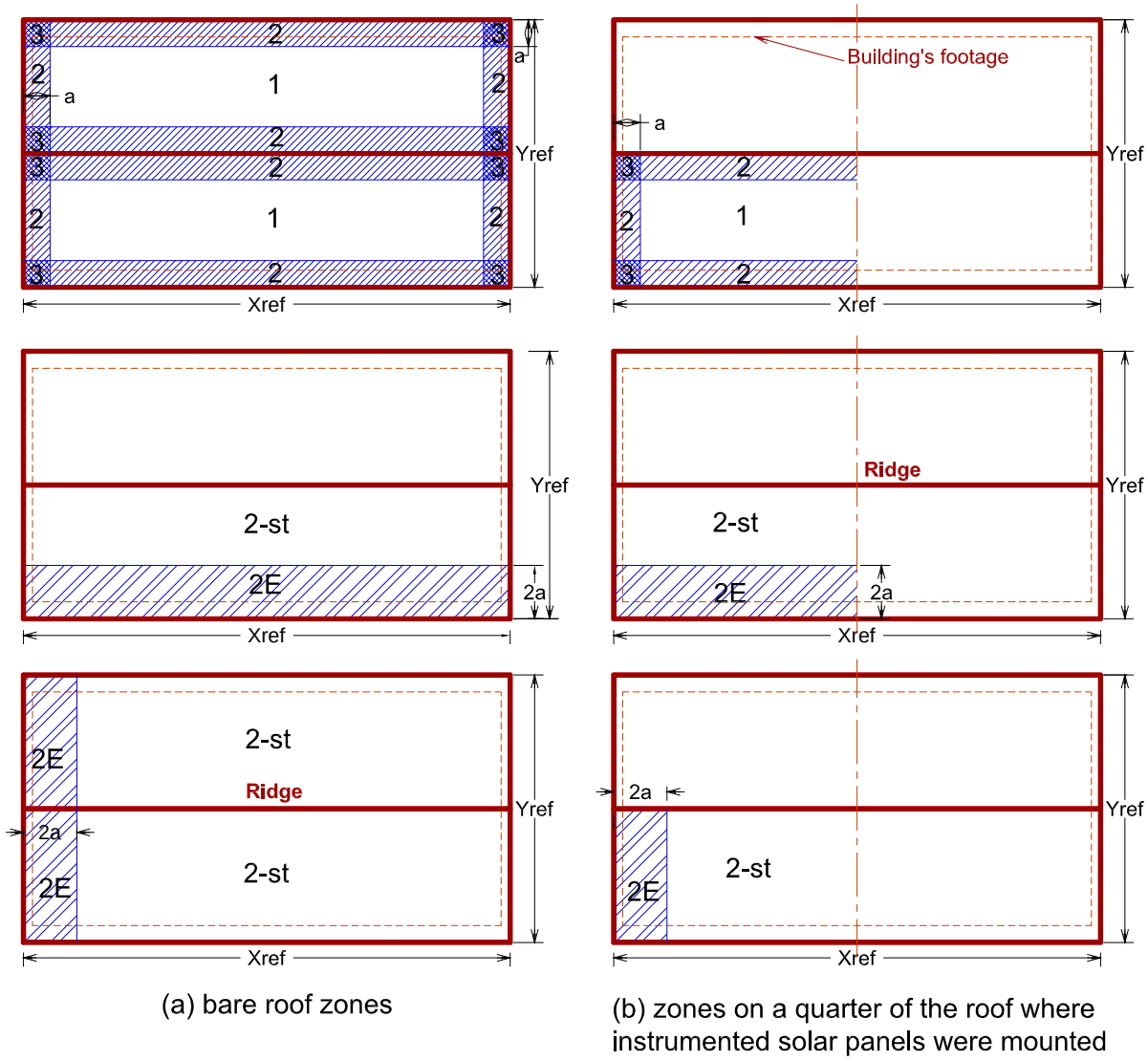

(a) bare roof zones

(b) zones on a quarter of the roof where instrumented solar panels were mounted

Fig. 10 Roof zones (3, 2 and 1) used for comparisons with data provided in the ASCE-2005 (Figure 6-11C of the standard) for claddings, and roof zones (2E and 2-st) used for comparisons with data provided the ASCE (Figure 6-10 of the standard) for the main force resisting system: (a) zones over a bare gable roof and (b) zones over the instrumented solar panel modules on a quarter of the same gable roof. Note that only quarter of the roof was instrumented due to symmetry.

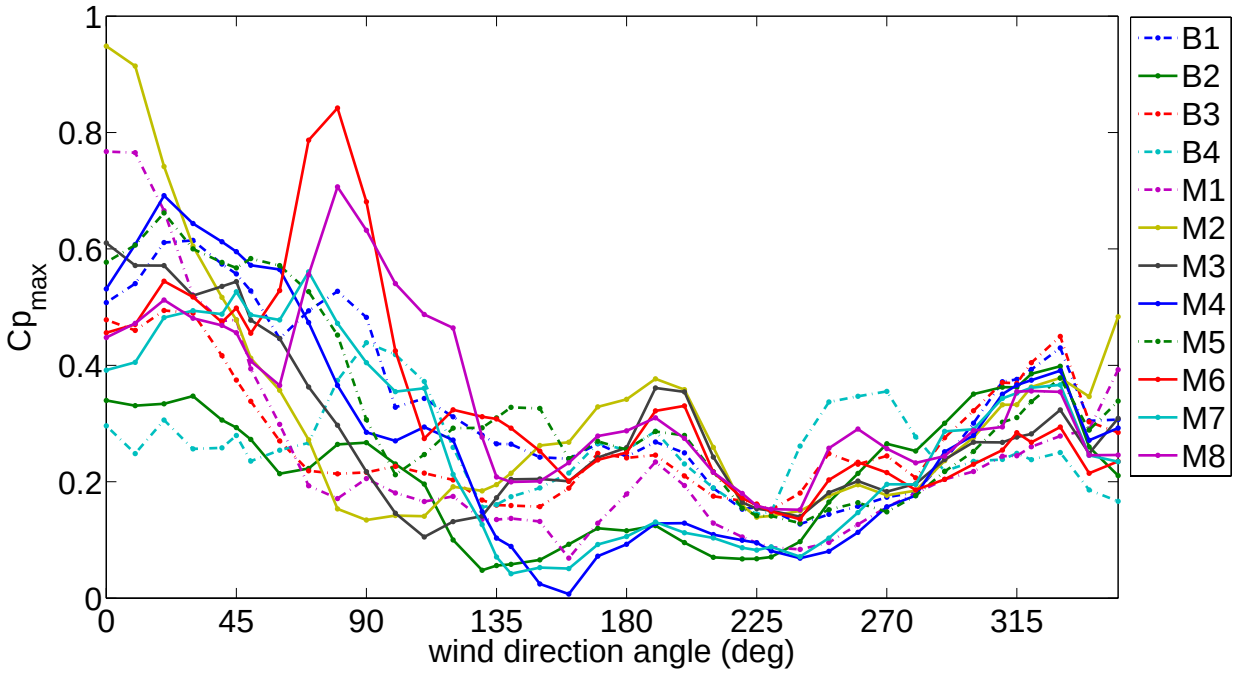

(a)

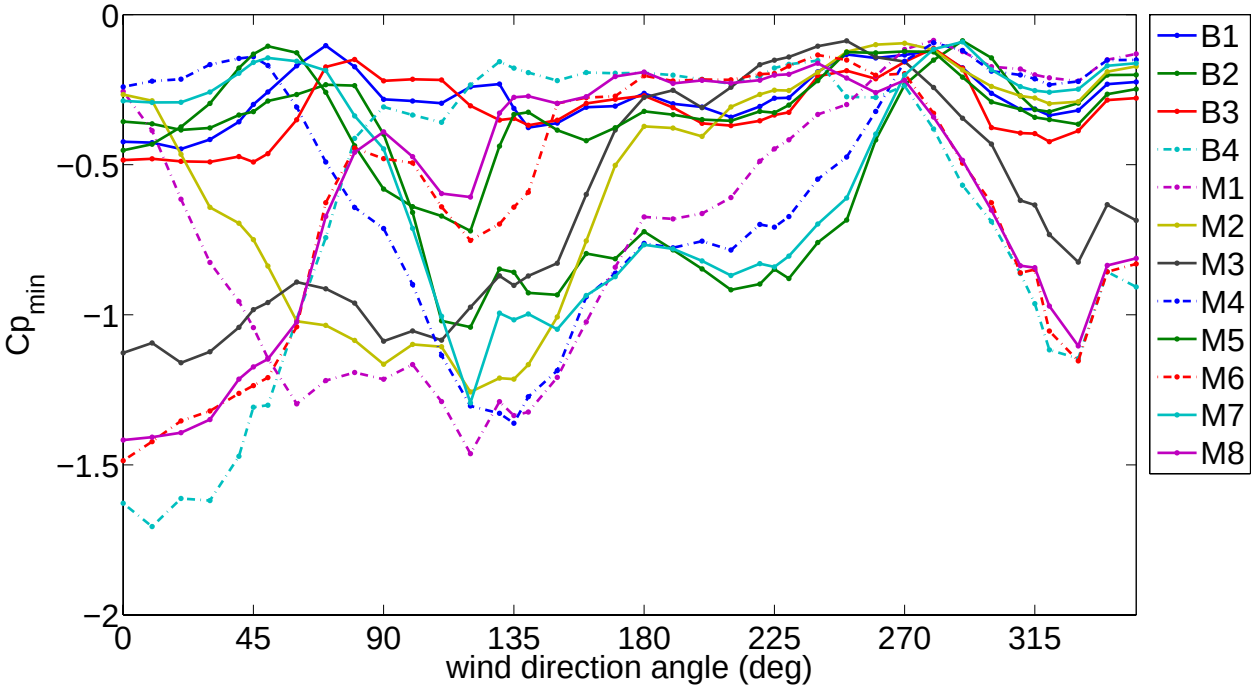

(b)

Fig. 11 Net pressure coefficients on solar panels mounted on a gable roof with slope 3:12 (14^o) for different wind direction angles: (a) maximum Cp and (b) minimum Cp.

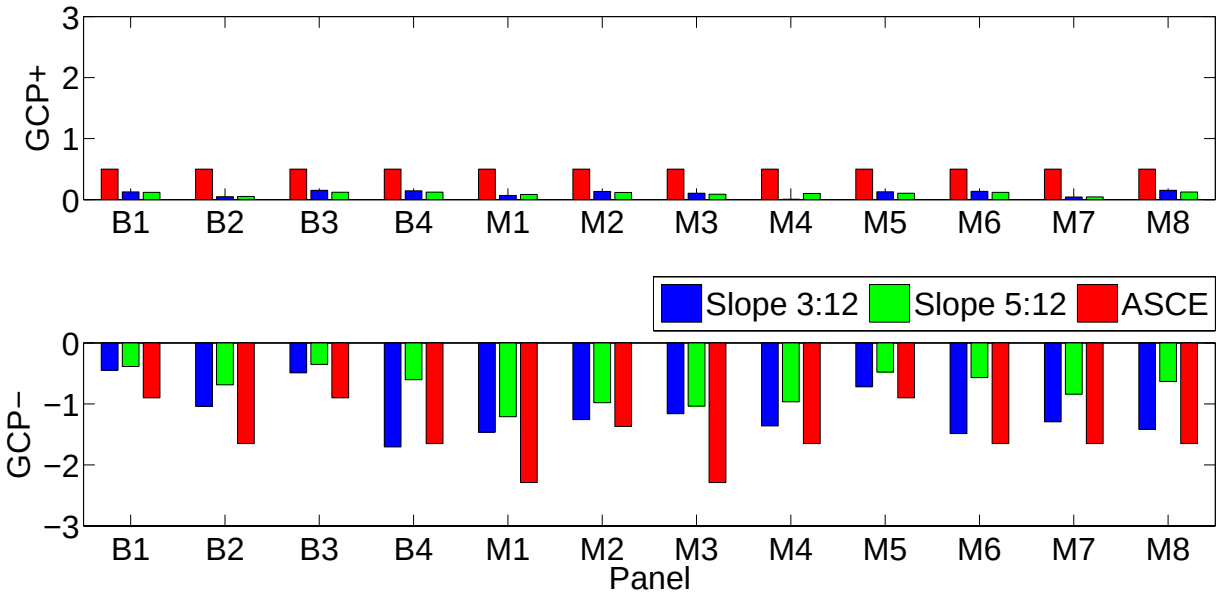

Fig. 12 Maximum and minimum pressure coefficients on solar panel modules mounted on gable roofs with slopes 3:12 (14^o) and 5:12 (22.6^o) in "configuration H1" of Fig. 2 and comparisons with coefficients obtained from external pressures on a bare gable roof as provided in the ASCE 7-2005 standard (7^o < slope < 27^o).

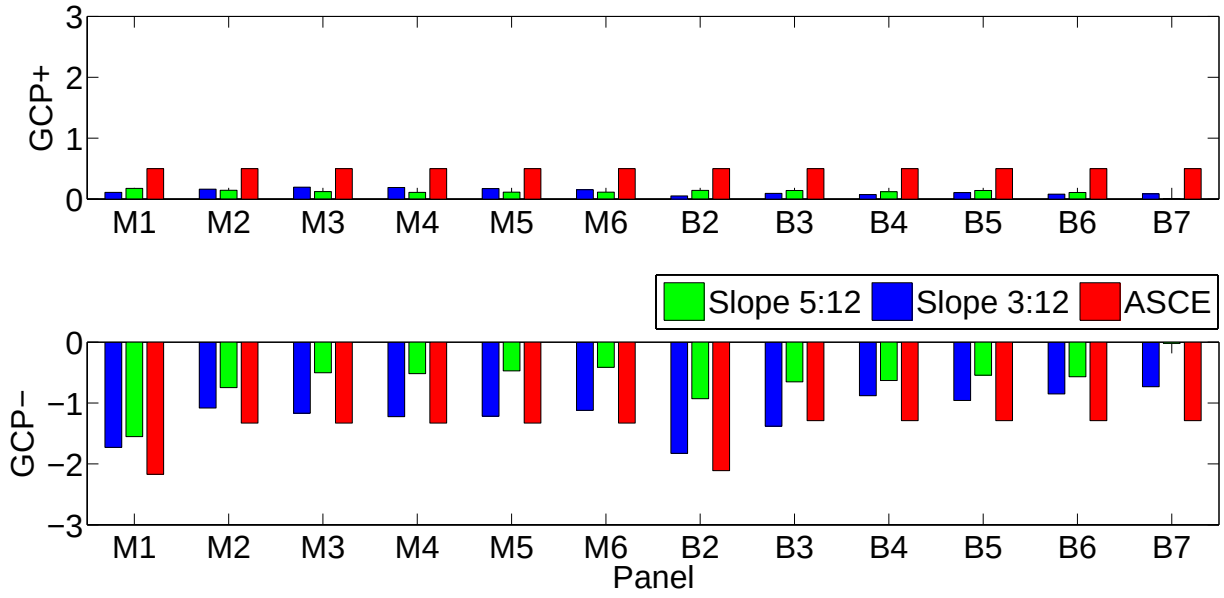

Fig. 13 Maximum and minimum pressure coefficients on solar panel modules mounted on gable roofs with slopes 3:12 (14^o) and 5:12 (22.6^o) in "configuration V1" of Fig. 2 and comparisons with coefficients obtained from external pressures on a bare gable roof as provided in the ASCE 7-2005 standard (7^o < slope < 27^o).

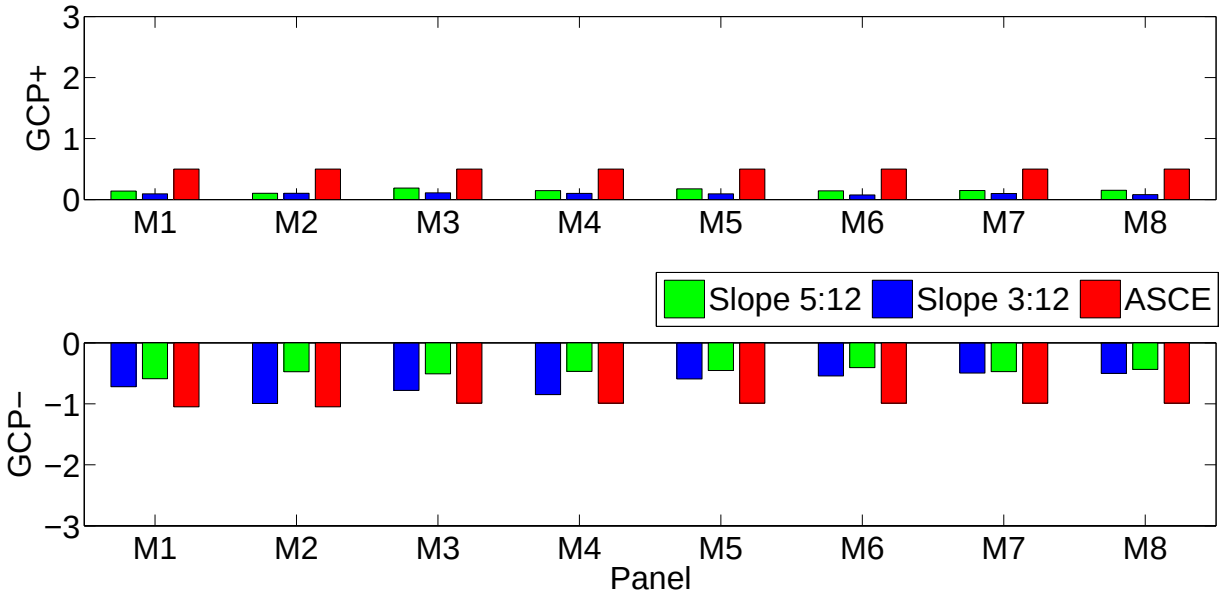

Fig. 14 Maximum and minimum pressure coefficients on solar panel modules mounted on gable roofs with slopes 3:12 (14^o) and 5:12 (22.6^o) in "configuration H2" of Fig. 2 and comparisons with coefficients obtained from external pressures on a bare gable roof as provided in the ASCE 7-2005 standard (7^o < slope < 27^o).

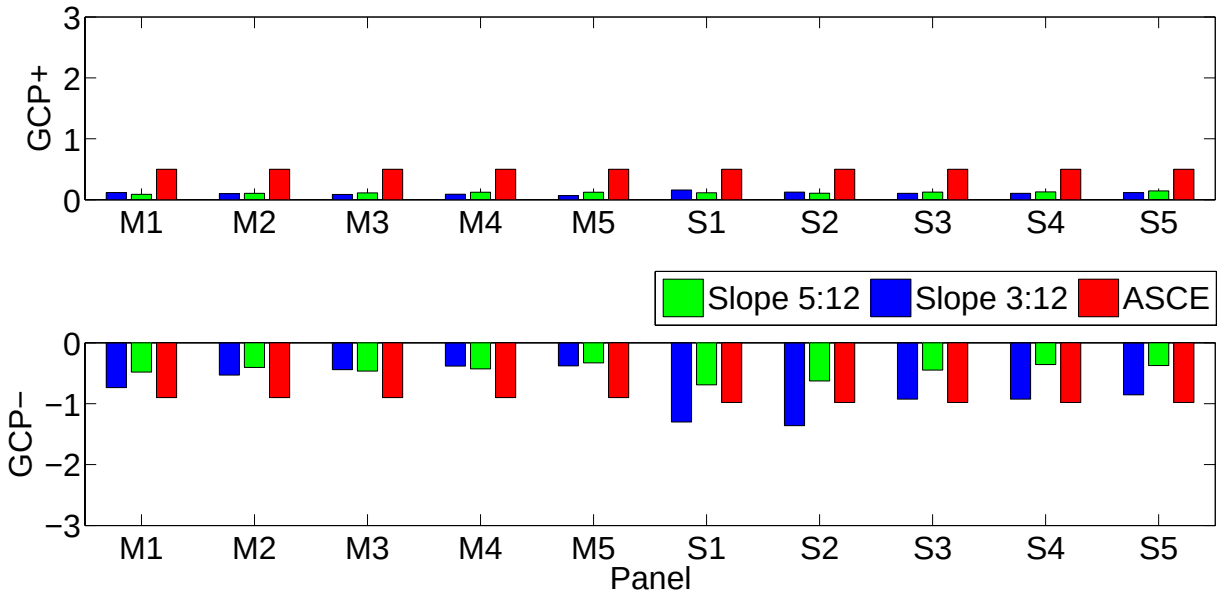

Fig. 15 Maximum and minimum pressure coefficients on solar panel modules mounted on gable roofs with slopes 3:12 (14^o) and 5:12 (22.6^o) in "configuration V2" of Fig. 2 and comparisons with coefficients obtained from external pressures on a bare gable roof as provided in the ASCE 7-2005 standard (7^o < slope < 27^o).